Sultanov, Aidar; Kuzmanović, Marko; Lebedev, Andrey V.; Paraoanu, Gheorghe Sorin

Protocol for temperature sensing using a three-level transmon circuit

Published in:
Applied Physics Letters

DOI:
10.1063/5.0065224

Published: 04/10/2021

Document Version
Publisher's PDF, also known as Version of record

Please cite the original version:
Sultanov, A., Kuzmanović, M., Lebedev, A. V., & Paraoanu, G. S. (2021). Protocol for temperature sensing using a three-level transmon circuit. *Applied Physics Letters*, *119*(14), Article 144002.
https://doi.org/10.1063/5.0065224

Applied Physics Letters

Protocol for temperature sensing using a three-level transmon circuit

Cite as: Appl. Phys. Lett. **119**, 144002 (2021); https://doi.org/10.1063/5.0065224
Submitted: 30 July 2021 • Accepted: 17 September 2021 • Published Online: 06 October 2021

Aidar Sultanov, Marko Kuzmanović, Andrey V. Lebedev, et al.

Applied Physics Letters ARTICLE scitation.org/journal/apl

Protocol for temperature sensing using a three-level transmon circuit

Cite as: Appl. Phys. Lett. **119**, 144002 (2021); doi: 10.1063/5.0065224
Submitted: 30 July 2021 · Accepted: 17 September 2021 ·
Published Online: 6 October 2021

View Online Export Citation CrossMark

Aidar Sultanov,[1] Marko Kuzmanović,[1] Andrey V. Lebedev,[2,3] and Gheorghe Sorin Paraoanu[1,a)]

AFFILIATIONS

[1]QTF Centre of Excellence, Department of Applied Physics, School of Science, Aalto University, FI-00076 Aalto, Finland
[2]Dukhov Research Institute of Automatics (VNIIA), Moscow 127055, Russia
[3]Moscow Institute of Physics and Technology, 141700, Institutskii Per. 9, Dolgoprudny, Moscow Region, Russia

Note: This paper is part of the APL Special Collection on Emerging Qubit Systems - Novel Materials, Encodings and Architectures.
[a)]**Author to whom correspondence should be addressed:** sorin.paraoanu@aalto.fi

ABSTRACT

We present a method for *in situ* temperature measurement of superconducting quantum circuits, by using the first three levels of a transmon device to which we apply a sequence of π gates. Our approach employs projective dispersive readout and utilizes the basic properties of the density matrix associated with thermal states. This method works with an averaging readout scheme and does not require a single-shot readout setup. We validate this protocol by performing thermometry in the range of 50–200 mK, corresponding to a range of residual populations 1%–20% for the first excited state and 0.02%–3% for the second excited state.

Superconducting qubits are one of the most promising candidates as the basic element of future quantum computers. The progress of the last decade has resulted in a significant increase in their coherence times to tens of microseconds,[1–3] in a reduction of errors caused by interaction with the environment through the implementation of reset protocols[4–9] and error-correction protocols[10,11] and in an enhancement in readout fidelity up to 99.6%.[12–15] However, the exact mechanisms that limit further improvements in superconducting qubit systems are still not fully understood; one possibility is the spurious excitations caused by microwave noise, infrared radiation from hotter stages of the dilution refrigerators or poisoning by quasiparticles.[16–19] To mitigate these effects, a range of experimental techniques have been deployed—the use of cryogenic filters and attenuators, infrared absorbers, radiation and magnetic shielding of samples, with the goal of reducing the temperature of the electromagnetic environment and the quasiparticle population. Here, we introduce a protocol for evaluating the effective temperature of a superconducting qubit. Our method can be readily used as a diagnostic tool for qubit thermalization and line integrity in quantum computing applications. An important application is quantum thermodynamics,[20–22] where controlling the effective temperature of the circuit can be used to drive quantum engines.

The state of the electromagnetic environment of the qubit is described by an effective temperature, which characterizes the thermal equilibrium between the qubit and the environment and, thus, defines residual populations of former. There are several ways to estimate this effective temperature from the residual populations of qubit's states, assuming a Maxwell–Boltzmann distribution. A straightforward method is to use a single-shot readout. In this case, the residual probabilities can be directly calculated from measurement statistics, provided that the states can be discriminated with sufficiently good precision. Another technique, also based on single-shot readout, uses the correlations between responses corresponding to the ground and excited states.[23] However, the implementation of a single-shot readout scheme requires a good quantum limited parametric amplifier and additional components.[24–26] An alternative approach uses a three level system, where the Rabi oscillation amplitude between the first and the second excited state depends on the residual population of the first excited state.[4,27] However, this method is highly sensitive to the readout signal parameters. Finally, a thermometry technique for propagating waves in open-waveguides[28] can be used to characterize the temperature of the electromagnetic field, but this method requires a dedicated sample design.

Here, we propose an *in situ* method for measuring the effective temperature, which utilizes only π pulses and requires measuring only the average responses in the dispersive readout limit. Therefore, this method could be implemented without a specialized setup or sophisticated measurement techniques. In addition, determining the temperature does not rely on qubit state tomography: In our protocol, we measure the cavity responses after applying six different drive sequences that swap the populations of the three-level system, in our case defined by the first levels in a transmon device. A simple linear relationship is found between some of these responses, and the coefficient of proportionality is determined only by the thermal level occupations. Therefore, as the method does not rely on full state tomography or on the knowledge of the pure state responses, it is more resilient to noise and drifts, which are commonly present in superconducting artificial atom experiments. Moreover, since only π pulses are utilized, the proposed method is robust against dephasing and, if the pulses are much shorter with respect to the relaxation time, also against decay.

Consider a three-level system in thermal equilibrium with its environment at a temperature T. The density matrix reads

$$\hat{\rho} = p_e\,|g\rangle\langle g| + p_e|e\rangle\langle e| + p_f\,|f\rangle\langle f| \tag{1}$$

where $|\langle g,\ |e\rangle,\ |f\rangle$ are, respectively, the ground, the first excited, and the second excited states, with corresponding populations p_g, p_e, and p_f. Thermal equilibrium means that $\hat{\rho}$ is diagonal, and the residual populations are defined by the Maxwell–Boltzmann distribution

$$p_g = \frac{1}{Z}e^{-\frac{E_g}{k_B T}}, \quad p_e = \frac{1}{Z}e^{-\frac{E_e}{k_B T}}, \quad p_f = \frac{1}{Z}e^{-\frac{E_f}{k_B T}}, \tag{2}$$

where k_B is the Boltzmann constant, T is the effective temperature, E_i with $i \in \{g, e, f\}$ are the energies of the corresponding states, and $Z = \sum_i \exp[-E_i/k_BT]$ is the canonical partition function.

For a transmon device, the readout of these three levels is implemented through the projective measurement operators[29]

$$\widehat{M_I} = \varphi_g^I|g\rangle\langle g| + \varphi_e^I|e\rangle\langle e| + \varphi_f^I|f\rangle\langle f|, \tag{3a}$$

$$\widehat{M_Q} = \varphi_g^Q|g\rangle\langle g| + \varphi_e^Q|e\rangle\langle e| + \varphi_f^Q|f\rangle\langle f|, \tag{3b}$$

where $\widehat{M_I}$, $\widehat{M_Q}$ are measurement operators, corresponding to the I and Q quadratures of the measured signal: These quadratures are denoted by $\varphi_i^{I(Q)}$ for the corresponding states. More precisely, in this formalism, $\varphi_i^{I(Q)}$ is the $I(Q)$ quadrature of the measured signal if the device is prepared in the state $|i\rangle$. Note that $\varphi_i^{I(Q)}$ are time-dependent functions, which makes the operators $\widehat{M_{I(Q)}}$ also time-dependent.

The averaged measurement result of an arbitrary state is defined as follows:

$$\begin{aligned}\langle I\rangle &= Tr\left(\hat{\rho}\widehat{M_I}\right),\\ \langle Q\rangle &= Tr\left(\hat{\rho}\widehat{M_Q}\right).\end{aligned} \tag{4}$$

For a thermal state $\hat{\rho}$, the measurement outcome becomes

$$\langle I\rangle = p_g\varphi_g^I + p_e\varphi_e^I + p_f\varphi_f^I, \tag{5a}$$

$$\langle Q\rangle = p_g\varphi_g^Q + p_e\varphi_e^Q + p_f\varphi_f^Q. \tag{5b}$$

If the pure state responses $\varphi_{g,e,f}^{I/Q}$ were known, one could in principle extract the thermal populations by linear regression. However, in the averaged readout scheme, only the ensemble average is accessible.

To overcome this difficulty, we propose to measure the responses after applying certain pulse sequences that swap the populations of three level systems in the density matrix Eq. (1). As we will see, the protocol allows us to eliminate completely the unknown responses $\varphi_i^{I(Q)}$. Let us denote the pulse swapping the ground and first excited state populations as π_{ge} and that swapping the first and second excited states as π_{ef}. All used sequenced are summarized in Table I. For example, when a single π_{ge} pulse is applied, one gets the state $\hat{\rho} = p_e\,|g\rangle\langle g| + p_g\,|e\rangle\langle e| + p_f\,|f\rangle\langle f|$, and according to Eq. (5), we get the output of the I-quadrature as $p_e\varphi_g^I(t) + p_g\varphi_e^I(t) + p_f\varphi_f^I(t)$. Here, we note that, in order to implement the protocol and the proposed sequences of gates, the second excited state should be accessible by dispersive readout.

In general, the responses $\varphi(t)_{g,e,f} = \varphi(t)_{g,e,f}^I + i\varphi(t)_{g,e,f}^Q$ can be understood as vectors in an infinite-dimensional (with respect to time) vector space over a complex $I + iQ$ field. For the sake of simplicity, from now on, we present all the expressions for the I and Q components separately. From this point of view, the differences of some of these responses can be classified according to the collinearity criterion. For example, the difference of $x_0^{I(Q)} - x_1^{I(Q)} = (p_g - p_e)(\varphi_g^{I(Q)} - \varphi_e^{I(Q)})$ and $y_0^{I(Q)} - y_1^{I(Q)} = (p_g - p_f)(\varphi_g^{I(Q)} - \varphi_e^{I(Q)})$ can be seen as two collinear vectors in the space spanned by $\varphi_{g,e,f}^{I,Q}$ and which lie along the direction $\varphi_{ge} = \varphi_g^{I(Q)} - \varphi_e^{I(Q)}$. Therefore, $x_0^{I(Q)} - x_1^{I(Q)} = (y_0^{I(Q)} - y_1^{I(Q)})\frac{p_g-p_e}{p_g-p_f}$, and it is possible to determine the coefficient of proportionality $A^{I(Q)} = \frac{p_g-p_e}{p_g-p_f}$ along the direction φ_{ge}, without knowledge of the pure state responses. Similarly, A is also the slope between either $y_0^{I(Q)} - x_2^{I(Q)}$ and $x_0^{I(Q)} - y_2^{I(Q)}$, along the direction φ_{gf} or the slope between $y_1^{I(Q)} - y_2^{I(Q)}$ and $x_1^{I(Q)} - x_2^{I(Q)}$ along the direction φ_{ef}.

Overall, we have identified the following pairs of differences:

$$\begin{cases} A = \dfrac{x_0^{I(Q)} - x_1^{I(Q)}}{y_0^{I(Q)} - y_1^{I(Q)}} = \dfrac{y_0^{I(Q)} - x_2^{I(Q)}}{x_0^{I(Q)} - y_2^{I(Q)}} = \dfrac{y_1^{I(Q)} - y_2^{I(Q)}}{x_1^{I(Q)} - x_2^{I(Q)}} = \dfrac{p_g - p_e}{p_g - p_f}, \\[2ex] B = \dfrac{x_1^{I(Q)} - y_1^{I(Q)}}{y_0^{I(Q)} - x_2^{I(Q)}} = \dfrac{x_2^{I(Q)} - y_2^{I(Q)}}{x_0^{I(Q)} - x_1^{I(Q)}} = \dfrac{x_0^{I(Q)} - y_0^{I(Q)}}{y_1^{I(Q)} - y_2^{I(Q)}} = \dfrac{p_e - p_f}{p_g - p_e}, \end{cases} \tag{6}$$

where column-wise ratios of responses are given along the directions of φ_{ge}, φ_{gf}, and φ_{ef}, correspondingly.

TABLE I. Sequences of operations used for the temperature measurement protocol.

Sequence	Outcome	Label
No pulses	$p_g\varphi_g^{I(Q)} + p_e\varphi_e^{I(Q)} + p_f\varphi_f^{I(Q)}$	$x_0^{I(Q)}$
π_{ge}	$p_e\varphi_g^{I(Q)} + p_g\varphi_e^{I(Q)} + p_f\varphi_f^{I(Q)}$	$x_1^{I(Q)}$
$\pi_{ge}\,\pi_{ef}$	$p_e\varphi_g^{I(Q)} + p_f\varphi_e^{I(Q)} + p_g\varphi_f^{I(Q)}$	$x_2^{I(Q)}$
π_{ef}	$p_g\varphi_g^{I(Q)} + p_f\varphi_e^{I(Q)} + p_e\varphi_f^{I(Q)}$	$y_0^{I(Q)}$
$\pi_{ef}\pi_{ge}$	$p_f\varphi_g^{I(Q)} + p_g\varphi_e^{I(Q)} + p_e\varphi_f^{I(Q)}$	$y_1^{I(Q)}$
$\pi_{ef}\pi_{ge}\,\pi_{ef}$	$p_f\varphi_g^{I(Q)} + p_e\varphi_e^{I(Q)} + p_g\varphi_f^{I(Q)}$	$y_2^{I(Q)}$

The coefficients of proportionality A and B are uniquely determined by the temperature T and the transition frequencies $\hbar\omega_{ge} = E_g - E_e$ and $\hbar\omega_{gf} = E_g - E_f$

$$\begin{cases} A = \dfrac{1-\exp\left(\hbar\omega_{ge}/k_{\mathrm{B}}T\right)}{1-\exp\left(\hbar\omega_{gf}/k_{\mathrm{B}}T\right)}, \\ B = \dfrac{\exp\left(\hbar\omega_{ge}/k_{\mathrm{B}}T\right)-\exp\left(\hbar\omega_{gf}/k_{\mathrm{B}}T\right)}{1-\exp\left(\hbar\omega_{ge}/k_{\mathrm{B}}T\right)}. \end{cases} \tag{7}$$

From Eq. (7), it is possible to determine the temperature T, assuming that the transition frequencies are known.

Note that in principle, one could introduce also the coefficient

$$C = \frac{x_1^{I(Q)} - y_1^{I(Q)}}{x_0^{I(Q)} - y_2^{I(Q)}} = \frac{x_2^{I(Q)} - y_2^{I(Q)}}{y_0^{I(Q)} - y_1^{I(Q)}} = \frac{x_0^{I(Q)} - y_0^{I(Q)}}{x_1^{I(Q)} - x_2^{I(Q)}}. \tag{8}$$

However, it is easily verified that

$$C = \frac{p_e - p_f}{p_g - p_f} = \frac{\exp\left(\hbar\omega_{ge}/k_{\mathrm{B}}T\right) - \exp\left(\hbar\omega_{gf}/kT\right)}{1-\exp\left(\hbar\omega_{gf}/k_{\mathrm{B}}T\right)}, \tag{9}$$

therefore, $C = A * B$, and therefore, it does not provide an independent measure of the temperature but can be used to estimate the accuracy of the protocol, which is discussed further in the supplementary material. Finally, we note that the protocol uses only π pulses; therefore, it should be insensitive to qubit dephasing and to a large extent also to qubit relaxation, since the duration of the π pulse is typically much smaller than the T_1 time.

Based on this protocol, we implement two experiments using a standard low-temperature cryogenic setup with microwave wiring for input lines and with a heterodyne readout. The samples consist of a transmon device coupled to a microwave coplanar resonator, which is used for dispersive readout. The energy levels of the transmon can be flux-tuned through a filtered DC flux bias line. The sample is thermally anchored to the mixing chamber of a dilution refrigerator and isolated from the output line by two circulators working in the 4 − 8 GHz range. The readout pulse duration is 2 μs, and the transmitted signal is amplified by 30 dB with a cryogenic amplifier at the 4.2 K stage and by room-temperature amplifiers by 60 dB. After the demodulation to an IF frequency of 50 MHz, the in-phase and quadrature components (IQ) are amplified by a low-bandwidth amplifier and digitized with 1 ns resolution with a data acquisition board (more information in the supplementary material). We calibrate the π pulses for e–g and e–f transitions by standard Rabi experiments, and we use them to define the sequences of the population swapping operations described in Table I. The excitation pulses are generated by an arbitrary waveform generator and mixed with a local oscillator (LO) frequency in an IQ mixer.

The pulses have Gaussian envelope and a duration between 56 and 120 ns, and the cross-excitation due to low transmon anharmonicity $f_{ge} - f_{ef} \approx 300$ MHz was negligible. We measure the response for each of the sequences, obtaining the IQ values of readout pulse. Each response is measured 60 000 times and averaged. The total attenuation is the same for both experiments and adds up to 75 and 73 dB for the readout and drive lines correspondingly. In the main text, the temperatures are determined using only the I quadrature data, while in the supplementary material, for the error estimations, both the I and Q data are used.

The goal of the first experiment is to test the protocol. We use a sample with $E_c/(2\pi) = 360$ MHz and $E_J^{\max}/(2\pi) = 10.013$ GHz, and the readout resonator at $f_r = 7.75$ GHz. For the drive and readout lines, we use an attenuation of 30 dB at the mixing chamber stage (MXC). The effective temperature is measured as a function of flux bias at fixed base MXC temperature.

The measured coefficient A^I is shown in Fig. 1. In this figure, each point is obtained from a measurement of four readout traces x_0^I, x_1^I, y_0^I, and y_1^I at a certain time. The differences $x_0^I - x_1^I$ and $y_0^I - y_1^I$ are shown in the inset, where the oscillations at the IF frequency clearly visible, with the time interval used for the linearity check delineated by dashed lines; further examples of measured responses could be found in the supplementary material. To extract the slopes, we implement the Deming regression approach,[30] which considers noise in both X and Y axes. This approach relies on the assumption that errors in two-variable models are independent and follow a normal distribution law. We find that the extracted slope value 0.9936 is very close to 1, as one could check from Eq. (7), which implies that we expect a low temperature, since $\lim_{T\to 0^+} A = \lim_{T\to 0^+} \frac{1-\exp\left(\hbar\omega_{ge}/k_{\mathrm{B}}T\right)}{1-\exp\left(\hbar\omega_{gf}/k_{\mathrm{B}}T\right)} = 1$.

In Fig. 2, we show the extracted temperatures as a function of flux bias (qubit frequency). The results are in a good agreement with the base temperature of refrigerator and lay in the range of earlier reported temperatures, measured by other methods.[4,23–27] In thermal equilibrium with the environment, characterized by flat spectrum, the temperature should not depend on the transmon frequency.[31] We see only a small variation of temperature, which proves that sample 1 is generally well thermalized and the applied pulse sequences do not

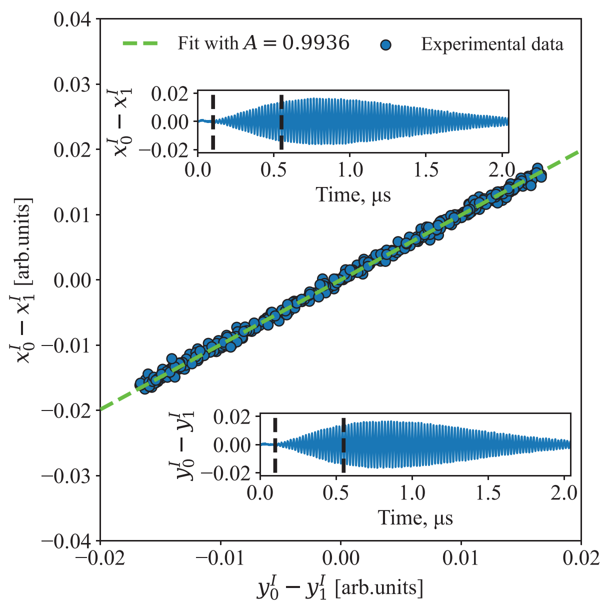

FIG. 1. Experimental verification of the linearity implied in Eq. (6). The bright green line is obtained by the linear regression algorithm resulting in a slope $A^I = 0.9936$. The plots show the differences between the I-quadrature time-domain traces $x_0^I - x_1^I$ and $y_0^I - y_1^I$, with the range of data used for extracting the slope shown by blue dashed lines in the insets. The raw data of readout signals are shown in the supplementary material.

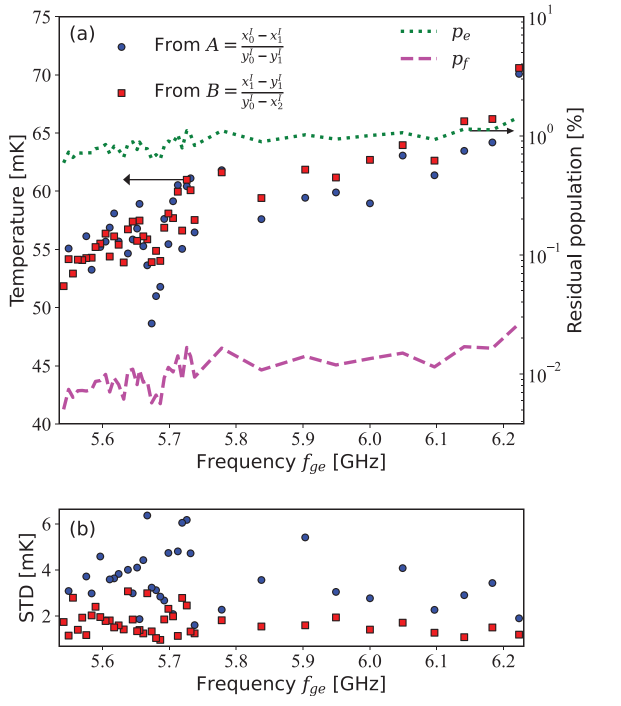

FIG. 2. (a) Effective temperature extracted from the responses A (blue circles) and B (red squares), see Eq. (6), for experiment 1 together with the residual populations of the state $|e\rangle$ (green dots) and $|f\rangle$ (magenta dashes). Note that the residual population on $|f\rangle$ remains below 0.03%. (b) Standard deviation of the effective temperature obtained from six realizations of each measurement.

influence it significantly. The slight dependence of the effective temperature could be explained by the frequency dependent attenuation of the control lines. The spikes near $\omega_{ge}/2\pi = 5.6 - 5.7$ GHz are most likely artifacts due to an imperfect calibration of π pulses.

The validity of our method is verified by a simulation of the system, where we model the Lindblad master equation with Boltzmann distribution for thermal photons; more details are presented in the supplementary material.

The goal in the second experiment is to demonstrate that the effective temperature can be controlled relatively independently from the temperature of the mixing chamber (MXC). The motivation comes from quantum thermodynamics, where superconducting-circuit based Otto engines[32] and Stirling engines[33] have been proposed theoretically. In these experiments, it would be useful to have access to and set in a straightforward way the temperature of two reservoirs, the hot and the cold one. Here, we show that by appropriate wiring we can have a relatively high temperature for the transmon, while at the same time maintaining the MXC as the cold bath.

For these measurements, we have used a sample with $E_c/(2\pi) = 350$ MHz and $E_J^{max}/(2\pi) = 20.412$ GHz, while the resonator frequency is $f_r = 4.906$ GHz. To achieve a higher effective temperature, the previous 30 dB of attenuation in the input line at the mixing chamber stage has been reduced by 15 dB, which results in a worse thermalization of the line and exposes the qubit to the thermal and non-equilibrium noise coming from the upper stages.[34] We observe an increase in the effective temperature of the transmon to about 160 mK.

Next, the effective temperature sensed by this sample is measured as a function of the base stage temperature; the results are shown in Fig. 3. We observe that the effective qubit temperature increases linearly with the MXC temperature. We have found that the slope in this linear dependence is approximately 1/3; therefore, $T_{eff} \approx T_{MXC}/3 + 155$ mK.

In the inset of Fig. 3, we present the results of monitoring the effective temperature at a fixed MXC temperature of 13 mK over 15 h. The temperature is roughly constant, except for the observation of a switching event at 7.5 h, most likely similar to the ones reported before in the literature.[19,35–39]

Above $T_{MXC} \approx 170$ mK, the effective temperatures estimated by A and B diverge. This can be understood as a consequence of the decreasing relaxation and coherence times at finite temperatures, and as a consequence the fidelities of drive and readout pulses decrease. To support this claim, we perform measurements of relaxation times. In Fig. 4, the relaxation times of the first and second excited states as a function of MXC temperatures are shown. Indeed, at MXC temperatures above 170 mK, the T_1 times drop significantly, which roughly coincides with the start of divergence seen in Fig. 3. This behavior is well explained by models taking into account quasiparticle generation, see, e.g., Refs. 19 and 40, which predict a drop in T_1 at temperatures very close to what we see in Fig. 4. A slight increase in the relaxation time for the second excited state has been observed in other experiments,[41] and it is explained by non-equilibrium quasiparticles.

In summary, we have proposed and demonstrated an *in situ* method to extract the temperature by applying a sequence of π gates to the first three levels of a transmon. The protocol is based on a standard setup, employing averaged readout for the transmon states, does

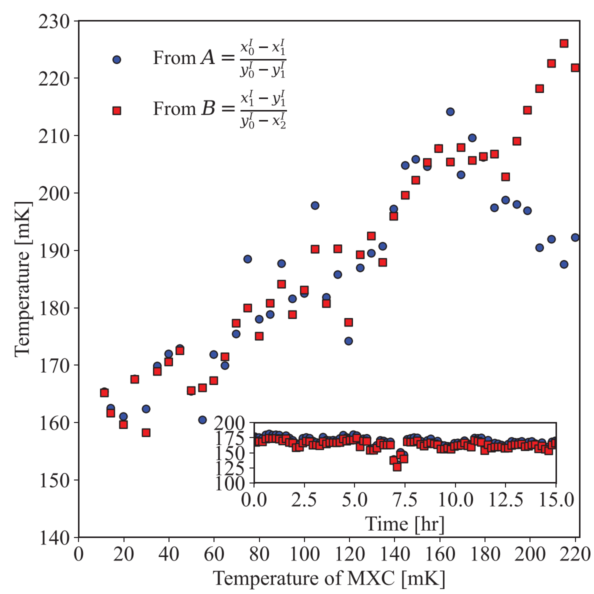

FIG. 3. The effective temperature in experiment 2 as a function of the base stage temperature (MXC). The inset shows the monitoring of effective temperature at a MXC temperature of 13 mK over 15 h, showing the appearance of jumps.

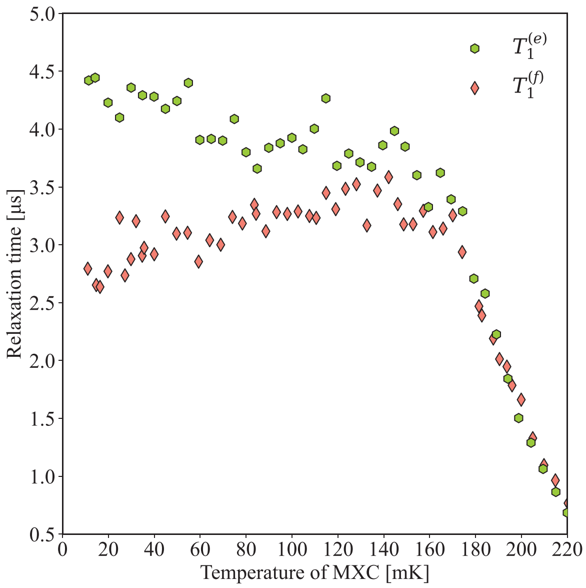

FIG. 4. The relaxation times of the first and second excited states, $T_1^{(e)}$ (green hexagonal symbol) and $T_1^{(f)}$ (salmon diamond symbol) as a function of MXC temperature.

not require single-shot measurements, and it is robust against certain types of noise, such as relaxation and decoherence. The extracted temperatures are in the expected range, agreeing with previously reported effective temperatures of the same type of qubits. We have also shown that this allows for either the diagnosis of thermal radiation coming from the hotter stages of the fridge or the use of this radiation as a thermal reservoir for thermodynamic quantum engines.

See the supplementary material that covers the details of the measurement procedure, a multilevel model of the transmon circuit including dissipation,[42,43] as well as a simulation of the temperature sensing protocol in the Qutip package.[44] Finally, a discussion of the main source of errors is presented.

The authors are grateful to Kirill Petrovnin and Shruti Dogra for assistance with the measurements and to Henrik Lievonen for help with data analysis. They acknowledge financial support from the RADDESS programme (Project No. 328193) of the Academy of Finland and from Grant No. FQXi-IAF19-06 ("Exploring the fundamental limits set by thermodynamics in the quantum regime") of the Foundational Questions Institute Fund (FQXi), a donor advised fund of the Silicon Valley Community Foundation. This work is part of the Finnish Center of Excellence in Quantum Technology QTF (Project Nos. 312296 and 336810) of the Academy of Finland. One of the samples used in this work was produced using the material and technical resources of the Common Use Center of the Research and Education Center "Functional Micro/Nanosystems" of the Bauman Moscow State Technical University. This work used the experimental facilities of the Low Temperature Laboratory of OtaNano and is part of the European Microkelvin Platform project, EMP (Grant Agreement No. 824109).

DATA AVAILABILITY

The data that support the findings of this study are available from the corresponding author upon reasonable request.

REFERENCES

[1]C. Rigetti, J. M. Gambetta, S. Poletto, B. L. T. Plourde, J. M. Chow, A. D. Córcoles, J. A. Smolin, S. T. Merkel, J. R. Rozen, G. A. Keefe, M. B. Rothwell, M. B. Ketchen, and M. Steffen, "Superconducting qubit in a waveguide cavity with a coherence time approaching 0.1 ms," Phys. Rev. B **86**, 100506(R) (2012).

[2]W. D. Oliver and P. B. Welander, "Materials in superconducting quantum bits," MRS Bull. **38**, 816 (2013).

[3]H. Paik, D. I. Schuster, L. S. Bishop, G. Kirchmair, G. Catelani, A. P. Sears, B. R. Johnson, M. J. Reagor, L. Frunzio, L. I. Glazman, S. M. Girvin, M. H. Devoret, and R. J. Schoelkopf, "Observation of high coherence in Josephson junction qubits measured in a three-dimensional circuit QED architecture," Phys. Rev. Lett. **107**, 240501 (2011).

[4]K. Geerlings, Z. Leghtas, I. M. Pop, S. Shankar, L. Frunzio, R. J. Schoelkopf, M. Mirrahimi, and M. H. Devoret, "Demonstrating a driven reset protocol for a superconducting qubit," Phys. Rev. Lett. **110**, 120501 (2013).

[5]S. O. Valenzuela, W. D. Oliver, D. M. Berns, K. K. Berggren, L. S. Levitov, and T. P. Orlando, "Microwave-induced cooling of a superconducting qubit," Science **314**, 1589 (2006).

[6]J. Tuorila, M. Partanen, T. Ala-Nissila, and M. Möttönen, "Efficient protocol for qubit initialization with a tunable environment," npj Quantum Inf. **3**, 27 (2017).

[7]D. Ristè, J. G. van Leeuwen, H.-S. Ku, K. W. Lehnert, and L. DiCarlo, "Initialization by measurement of a superconducting quantum bit circuit," Phys. Rev. Lett. **109**, 050507 (2012).

[8]D. J. Egger, M. Werninghaus, M. Ganzhorn, G. Salis, A. Fuhrer, P. Müller, and S. Filipp, "Pulsed reset protocol for fixed-frequency superconducting qubits," Phys. Rev. Appl. **10**, 044030 (2018).

[9]P. Magnard, P. Kurpiers, B. Royer, T. Walter, J.-C. Besse, S. Gasparinetti, M. Pechal, J. Heinsoo, S. Storz, A. Blais, and A. Wallraff, "Fast and unconditional all-microwave reset of a superconducting qubit," Phys. Rev. Lett. **121**, 060502 (2018).

[10]P. Campagne-Ibarcq, A. Eickbusch, S. Touzard, E. Zalys-Geller, N. E. Frattini, V. V. Sivak, P. Reinhold, S. Puri, S. Shankar, R. J. Schoelkopf, L. Frunzio, M. Mirrahimi, and M. H. Devoret, "Quantum error correction of a qubit encoded in grid states of an oscillator," Nature **584**, 368 (2020).

[11]M. D. Reed, L. DiCarlo, S. E. Nigg, L. Sun, L. Frunzio, S. M. Girvin, and R. J. Schoelkopf, "Realization of three qubit quantum error correction with superconducting circuits," Nature **482**, 382 (2012).

[12]R. Vijay, D. H. Slichter, and I. Siddiqi, "Observation of quantum jumps in a superconducting artificial atom," Phys. Rev. Lett. **106**, 110502 (2011).

[13]G. de Lange, D. Ristè, M. Tiggelman, C. Eichler, L. Tornberg, G. Johansson, A. Wallraff, R. Schouten, and L. DiCarlo, "Reversing quantum trajectories with analog feedback," Phys. Rev. Lett. **112**, 080501 (2014).

[14]Z. R. Lin, K. Inomata, W. D. Oliver, K. Koshino, Y. Nakamura, J. S. Tsai, and T. Yamamoto, "Single-shot readout of a superconducting flux qubit with a flux-driven Josephson parametric amplifier," Appl. Phys. Lett. **103**, 132602 (2013).

[15]B. Abdo, K. Sliwa, S. Shankar, M. Hatridge, L. Frunzio, R. Schoelkopf, and M. Devoret, "Josephson directional amplifier for quantum measurement of superconducting circuits," Phys. Rev. Lett. **112**, 167701 (2014).

[16]A. D. Córcolesa, J. M. Chow, J. M. Gambetta, C. Rigetti, J. R. Rozen, G. A. Keefe, M. B. Rothwell, M. B. Ketchen, and M. Steffen, "Protecting superconducting qubits from radiation," Appl. Phys. Lett. **99**, 181906 (2011).

[17]J. Wenner, Y. Yin, E. Lucero, R. Barends, Y. Chen, B. Chiaro, J. Kelly, M. Lenander, M. Mariantoni, A. Megrant, C. Neill, P. J. J. O'Malley, D. Sank, A. Vainsencher, H. Wang, T. C. White, A. N. Cleland, and J. M. Martinis, "Excitation of superconducting qubits from hot nonequilibrium quasiparticles," Phys. Rev. Lett. **110**, 150502 (2013).

[18]R. Barends, J. Wenner, M. Lenander, Y. Chen, R. C. Bialczak, J. Kelly, E. Lucero, P. O'Malley, M. Mariantoni, D. Sank, H. Wang, T. C. White, Y. Yin, J. Zhao, A. N. Cleland, J. M. Martinis, and J. J. A. Baselmans, "Minimizing

quasiparticle generation from stray infrared light in superconducting quantum circuits," Appl. Phys. Lett. **99**, 113507 (2011).
[19]K. Serniak, M. Hays, G. de Lange, S. Diamond, S. Shankar, L. D. Burkhart, L. Frunzio, M. Houzet, and M. H. Devoret, "Hot non-equilibrium quasiparticles in transmon qubits," Phys. Rev. Lett. **121**, 157701 (2018).
[20]J. P. Pekola, "Towards quantum thermodynamics in electronic circuits," Nat. Phys. **11**, 118 (2015).
[21]M. P. Silveri, J. A. Tuorila, E. V. Thuneberg, and G. S. Paraoanu, "Quantum systems under frequency modulation," Rep. Prog. Phys. **80**, 056002 (2017).
[22]M. Cattaneo and G. S. Paraoanu, "Engineering dissipation with resistive elements in circuit quantum electrodynamics," arXiv:2103.16946 (2021).
[23]A. Kulikov, R. Navarathna, and A. Fedorov, "Measuring effective temperatures of qubits using correlations," Phys. Rev. Lett. **124**, 240501 (2020).
[24]J. E. Johnson, C. Macklin, D. H. Slichter, R. Vijay, E. B. Weingarten, J. Clarke, and I. Siddiqi, "Heralded state preparation in a superconducting qubit," Phys. Rev. Lett. **109**, 050506 (2012).
[25]D. Ristè, C. C. Bultink, K. W. Lehnert, and L. DiCarlo, "Feedback control of a solid-state qubit using high-fidelity projective measurement," Phys. Rev. Lett. **109**, 240502 (2012).
[26]P. Krantz, A. Bengtsson, M. Simoen, S. Gustavsson, V. Shumeiko, W. D. Oliver, C. M. Wilson, P. Delsing, and J. Bylander, "Single-shot read-out of a superconducting qubit using a Josephson parametric oscillator," Nat. Commun. **7**, 11417 (2016).
[27]X. Y. Jin, A. Kamal, A. P. Sears, T. Gudmundsen, D. Hover, J. Miloshi, R. Slattery, F. Yan, J. Yoder, T. P. Orlando, S. Gustavsson, and W. D. Oliver, "Thermal and residual excited-state population in a 3D transmon qubit," Phys. Rev. Lett. **114**, 240501 (2015).
[28]M. Scigliuzzo, A. Bengtsson, J.-C. Besse, A. Wallraff, P. Delsing, and S. Gasparinetti, "Primary thermometry of propagating microwaves in the quantum regime," Phys. Rev. X **10**, 041054 (2020).
[29]R. Bianchetti, S. Filipp, M. Baur, J. M. Fink, C. Lang, L. Steffen, M. Boissonneault, A. Blais, and A. Wallraff, "Control and tomography of a three level superconducting artificial atom," Phys. Rev. Lett. **105**, 223601 (2010).
[30]W. E. Deming, *Statistical Adjustment of Data* (Wiley, 1943).
[31]A. A. Clerk, M. H. Devoret, S. M. Girvin, F. Marquardt, and R. J. Schoelkopf, "Introduction to quantum noise, measurement, and amplification," Rev. Mod. Phys. **82**, 1155 (2010).
[32]B. Karimi and J. P. Pekola, "Otto refrigerator based on a superconducting qubit: Classical and quantum performance," Phys. Rev. B **94**, 184503 (2016).
[33]S. H. Raja, S. Maniscalco, G. S. Paraoanu, J. P. Pekola, and N. L. Gullo, "Finite-time quantum Stirling heat engine," New J. Phys. **23**, 033034 (2021).
[34]S. Krinner, S. Storz, P. Kurpiers, P. Magnard, J. Heinsoo, R. Keller, J. Lutolf, C. Eichler, and A. Wallraff, "Engineering cryogenic setups for 100-qubit scale superconducting circuit systems," EPJ Quantum Technol. **6**, 2 (2019).
[35]L. Grünhaupt, N. Maleeva, S. T. Skacel, M. Calvo, F. Levy-Bertrand, A. V. Ustinov, H. Rotzinger, A. Monfardini, G. Catelani, and I. M. Pop, "Loss mechanisms and quasiparticle dynamics in superconducting microwave resonators made of thin-film granular aluminum," Phys. Rev. Lett. **121**, 117001 (2018).
[36]D. Ristè, C. C. Bultink, M. J. Tiggelman, R. N. Schouten, K. W. Lehnert, and L. DiCarlo, "Millisecond charge-parity fluctuations and induced decoherence in a superconducting transmon qubit," Nat. Commun. **4**, 1913 (2013).
[37]S. Schlör, J. Lisenfeld, C. Müller, A. Bilmes, A. Schneider, D. P. Pappas, A. V. Ustinov, and M. Weides, "Correlating decoherence in transmon qubits: Low frequency noise by single fluctuators," Phys. Rev. Lett. **123**, 190502 (2019).
[38]J. J. Burnett, A. Bengtsson, M. Scigliuzzo, D. Niepce, M. Kudra, P. Delsing, and J. Bylander, "Decoherence benchmarking of superconducting qubits," npj Quantum Inf. **5**, 54 (2019).
[39]C. R. H. McRae, G. M. Stiehl, H. Wang, S.-X. Lin, S. A. Caldwell, D. P. Pappas, J. Mutus, and J. Combes, "Reproducible coherence characterization of superconducting quantum devices," Appl. Phys. Lett. **119**, 100501 (2021).
[40]G. Catelani, J. Koch, L. Frunzio, R. J. Schoelkopf, M. H. Devoret, and L. I. Glazman, "Quasiparticle relaxation of superconducting qubits in the presence of flux," Phys. Rev. Lett. **106**, 077002 (2011).
[41]J. M. Martinis, M. Ansmannand, and J. Aumentado, "Energy decay in superconducting Josephson-junction qubits from nonequilibrium quasiparticle excitations," Phys. Rev. Lett. **103**, 097002 (2009).
[42]J. Koch, T. M. Yu, J. Gambetta, A. A. Houck, D. I. Schuster, J. Majer, A. Blais, M. H. Devoret, S. M. Girvin, and R. J. Schoelkopf, "Charge-insensitive qubit design derived from Cooper pair box," Phys. Rev. A **76**, 042319 (2007).
[43]K. S. Kumar, A. Vepsäläinen, S. Danilin, and G. S. Paraoanu, "Stimulated Raman adiabatic passage in a three-level superconducting circuit," Nat. Commun. **7**, 10628 (2016).
[44]J. R. Johansson, P. D. Nation, and F. Nori, "QuTiP 2: A Python framework for the dynamics of open quantum systems," Comput. Phys. Commun. **184**, 1234 (2013).